Reaction Pathways in the Liquid Phase Alkylation of Biomass-Derived Phenolic Compounds

Miguel Ángel González-Borja and Daniel E. Resasco
School of Chemical, Biological and Materials Engineering and Center for Interfacial Reaction Engineering, University of Oklahoma, Norman, OK 73019

DOI 10.1002/aic.14658
Published online November 5, 2014 in Wiley Online Library (wileyonlinelibrary.com)

Alkylation is a promising reaction for the upgrading of bio-oil because it maximizes the retention of carbon in the liquid product. The alkylation of m-cresol with isopropanol and HY zeolite was studied in a liquid phase system. The experimental results were fitted with two conventional surface kinetic models, Langmuir–Hinshelwood and Eley–Rideal, from which adsorption and rate constants were estimated. Two types of alkylation reactions were observed: C-alkylation with formation of a C—C bond with the ring and O-alkylation with formation of an ether bond with the hydroxyl group. It was concluded that O-alkylation products do not undergo intramolecular rearrangement but first decompose into the corresponding phenolic. Alkylation occurs from both isopropanol and propylene, both of them yielding O-and C-alkylation to different extents. Isopropanol favors O-alkylation while propylene favors C-alkylation. Rate constants for multiple alkylation steps were progressively lower, suggesting the presence of steric hindrance during incorporation of additional isopropyl groups. © 2014 American Institute of Chemical Engineers *AIChE J*, 61: 598–609, 2015
Keywords: alkylation, biomass conversion, isopropanol, kinetics, m-cresol

Introduction

Extensive research in utilization of biomass indicates that it is a promising feedstock for the sustainable production of fuels and chemicals.[1–3] Special emphasis has been given to the upgrading of bio-oil obtained from fast pyrolysis because it is a liquid product readily obtainable in large scale but highly susceptible to degradation with time and temperature. Upgrading and stabilization of bio-oil is a challenging task because of its chemical complexity; it contains hundreds of compounds with multiple functional groups, most of them oxygenated.[4,5] Recently, we have proposed that direct production of bio-oil fractions containing specific groups of compounds, as opposed to production of whole bio-oil could be beneficial for upgrading.[6,7] By following this approach, a particular strategy for improving the properties of each fraction could be developed and the complexity due to the presence of multiple functional groups in the reaction system be significantly reduced. Fractionation of bio-oil can be achieved either by a step-wise condensation of pyrolysis vapors or by a multistage pyrolysis process, in which each fraction is obtained from treating biomass at different temperatures and times. In this way, separate fractions with high concentration of light oxygenates (acids, aldehydes, ketones), sugar derived compounds, and phenolics can be obtained, respectively.

Small oxygenates can undergo ketonization that yields longer chain ketones,[8,9] which on hydrogenation produce secondary alcohols. For instance, isopropanol, derived from acetone, is an excellent alkylating agent that can be combined with the phenolics fraction from the bio-oil to generate alkylphenols in the C10–C13 range.[10] These compounds not only fall in the desirable carbon-chain fuel range but also are widely used as chemical intermediates in the synthesis of antioxidants, fragrances, agrochemicals, and fuel additives.[11–13] In bio-oil upgrading, it is desirable to conduct the reactions in the liquid phase as reheating the whole bio-oil or its fractions leads to an increase in the rate of degradation. However, the high water content of bio-oil presents a challenge for catalyst stability in liquid phase systems. In a recent study,[10] we have shown that alkylation of phenolic compounds with isopropanol in a biphasic system (aqueous and oil phases) can be successfully achieved using a hydrophobic HY zeolite with minimum zeolite degradation. This remarkable result is worth of further studies such as kinetic modeling, seeking to gain insight about reaction pathways and mechanisms. With this in mind, and with the objective of gaining fundamental understanding about this reaction, in this work we have simplified this system and studied the liquid phase alkylation in a single organic solvent, with no water present, and with a regular HY zeolite, without hydrophobization.

Alkylation of phenolic compounds has been widely studied during the last decades. Products like cresols, xylenols, isopropylphenols, and *tert*-butylphenols are of high value in the chemical industry and it is important to understand the processes and mechanisms by which they are obtained. It is well known that alkylation of phenolics can lead to either

Additional Supporting Information may be found in the online version of this article.

Correspondence concerning this article should be addressed to D. E. Resasco.at resasco@ou.edu

ring-alkylated products (C-alkylation) or ether products (O-alkylation). This is dependent on whether the alkylating agent is preferentially attacked by the electrons in the ring or the oxygen atom in the hydroxyl group, respectively. Selectivity toward a particular product has been attributed to a number of factors, including the type of catalytic site (acid or basic, strong or weak), reaction temperature and residence time, among others.[13–19] There have been numerous studies aiming to understand the mechanistic aspects of this reaction and even though it has not been yet clarified, there are some points of general agreement according to experimental observations and theoretical calculations. O-alkylation appears to occur at milder conditions as compared to C-alkylation, that is, lower temperatures,[16,17,20–23] short residence times, and weaker acid sites.[15,19] Experimentally, a change in selectivity toward C-alkylation products has been observed with an increase in temperature or residence time. The mechanism for this transformation is still a point of discussion, but it is believed that an alkyl-aryl ether can undergo intramolecular rearrangement to produce the respective alkylphenol.[23–25] This has lead to the conclusion that O-alkylation products are favored kinetically and are further converted into the more thermodynamically stables C-alkylation products.[25,26]

Some kinetics studies have favored an Eley–Rideal type mechanism for these alkylation reactions, in which the alkylating agent is adsorbed on the catalyst surface and reacts with a phenolic molecule from the bulk phase.[27–29]

In light of the potential application of this type of reactions in biomass utilization, we have performed a detailed kinetic study for the alkylation of m-cresol with isopropanol. Previous investigations have been limited to the use of simplified first- and second-order kinetics and have not considered surface coverage of reactants and products. In this study, we aim to understand the reaction pathways in this system and bring clarity to some of the mechanistic aspects discussed above. We do this with the help of a Langmuir–Hinshelwood kinetic model with inputs from independent measurements that enhance the robustness of the model. We have also compared this model with an Eley–Rideal type model, as this has previously been suggested to be the preferred mechanism for this reaction.

Experimental

The reactants used in this study were m-cresol (99%), 2-propanol (anhydrous, 99.5%), thymol (≥99.5%), all from Sigma-Aldrich, and isopropoxybenzene (IPB; 97%) from Oakwood Chemical. Propylene and He (ultra high purity) gases were obtained from airgas. All reactants were used as received, without further purification. Decahydronaphthalene, a mixture of cis + trans from Sigma-Aldrich (reagent grade, 98%) was used as the solvent. The catalyst used in the kinetics study was a HY zeolite from Zeolyst International (CBV 760) with a Si/Al ratio of 30, UCS 2.424 nm, SAR 720 $m^2\ g^{-1}$. Experiments were carried out in the liquid phase on a bench-top 0.3 L Parr pressure reactor (model 4561), equipped with a 4843 Parr controller for temperature, pressure, and stirring. In a typical experiment, the catalyst (20–50 mg) and the solvent (60 cm^3) were combined in a glass liner. Then, the solid was dispersed with the help of a horn sonicator (0.25 h at 25% amplitude). The liner was placed in the stainless steel reactor vessel and the system was purged and pressurized with He to 2.7 MPa. A separate solution containing m-cresol or thymol (0.0434 moles), isopropanol (0.0434–0.173 moles), and additional solvent (enough to complete a total reaction volume of 85 cm^3) was prepared. For reactions with IPB (0.0434 moles) no isopropanol was added. The temperature in the reactor was adjusted to the desired value. Then, the solution containing the feed was introduced in the reaction vessel by pressure difference from a separate vessel. When using propylene as the alkylating agent, the corresponding moles of gas where introduced at the same time as the liquid feed in the reactor. After injecting the feed, the pressure was adjusted to 4.8 MPa by adding He. The reaction was then performed in the batch mode for a given time in the closed vessel. Conversion data as a function of time were obtained with individual runs for each selected reaction time. At the end of each run, the liquid mixture was analyzed with a Shimadzu QP2010S gas chromatograph/mass spectrometer (GC-MS) to identify the products and a Varian 3800 gas chromatograph (GC) equipped with a flame ionization detector for quantification. Both GC's were equipped with a Zebron ZB-1701 column with dimensions of 60 m × 0.25 mm × 0.25 μm.

The Koros–Nowak/Madon–Boudart test[30] was used to determine whether the measured reaction rates were affected by the rate of mass transfer. For this test, the HY zeolite was sodium exchanged to a varying extent to generate samples with the same crystallite size but with different acid site concentrations. In particular, the 1 g of zeolite powder, with a theoretical acid density of 538 μmol g^{-1}, was exchanged with 50 cm^3 of a sodium hydroxide solution containing enough base to neutralize 12% and 19% of the theoretical acid sites. The solution was stirred for 24 h at room temperature and then the solids were separated by centrifugation and dried overnight at 373 K. The acid site density of the original zeolite and the resulting residual acidity of the exchanged samples were measured using thermal programmed desorption (TPD) of isopropylamine, as described elsewhere.[31] Briefly, the TPD system consists of a $1/4''$ quartz tube inside a tubular furnace and a MKS Cirrus MS. During each run, the MS scans the following fractions (m/z) at a rate of 1 scan/s: 4, 16, 17, 18, 28, 32, 41, 44, and 58. The system has the capability for injecting liquids through a rubber septum and gases through a 6-port valve into a stream of preheated He carrier gas. The system was calibrated using 10 pulses of propylene through an empty quartz tube. For the TPD run, a constant flow of He was kept at 20 $cm^3\ min^{-1}$; the zeolite (50 mg) was placed in the quartz tube and pretreated for 2 h at 673 K and then overnight at 373 K. Adsorption of isopropylamine at 373 K was accomplished by multiple 2 μL injections, until saturation of the catalyst was confirmed in the MS. Following the injections, the samples were purged in He at the same temperature for 4 h to remove weakly adsorbed isopropylamine. Finally, the desorption was measured under a heating ramp of 10 K min^{-1} in the 373–873 K range. The moles of propylene evolved during TPD were correlated to the concentration of Brønsted acid sites in the catalyst, following Gorte's method.[32]

Microsoft Excel was used as the software for kinetic modeling. Using initial estimates for the model parameters, the concentration of each species was estimated at differential time intervals. Then, a least squares methodology was implemented with the help of the Excel tool Solver to find the parameter values that best fit the experimental data. As it will be explained below, a number of constraints were imposed on the model to ensure the estimated parameters were physically meaningful.

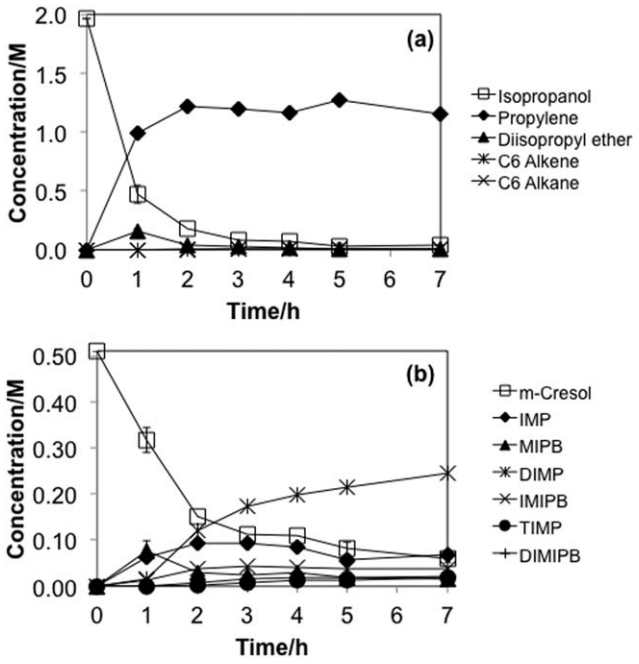

Figure 1. Product distribution from alkylation of m-cresol with isopropanol. (a) Dehydration/ oligomerization products. (b) Alkylation products.

Conditions: isopropanol/m-cresol = 3.8, $T = 473$ K, $P = 4.8$ MPa, catalyst mass = 50 mg HY. Error bars are shown only for experiments that were duplicated.

Results and Discussion

Product distribution from alkylation of m-cresol with isopropanol

The reaction between m-cresol and isopropanol was monitored as a function of time. As shown in Figure 1a, isopropanol rapidly converts, forming the dehydration products di-isopropyl ether and propylene. Although direct dehydration to propylene seems to be a significant path, it is clear that di-isopropyl ether also forms as a primary product and then decomposes to produce propylene and water. Subsequently, propylene undergoes oligomerization to form higher olefins, although in this case only methylpentenes were observed. Higher olefins are likely to stay on the surface and participate in the formation of coke.

Multiple alkylation products were identified by GC-MS. As summarized in Scheme 1, both C-alkylation (IMP, DIMP, TIMP) and O-alkylation (MIPB, IMIPB, DIMIPB) products were formed under the reaction conditions investigated. Only IMP and DIMP could be directly matched to a registry in the mass spectrometer library. Therefore, the other products were identified by analyzing the observed fragmentation patterns. In general, ethers tend to cleave at the oxygen–carbon bond, in this case releasing an isopropyl fragment with m/z of 42. Likewise, we anticipate that the main fragmentation observed in the ring-alkylated products should result from C—C cleavage and release a methyl fragments with m/z of 15. These simple fragmentation rules were sufficient for distinguishing ethers from ring-alkylated products. Notice that this analysis does not differentiate among the specific isomers produced. Therefore, they are lumped together, with the acknowledgment that isomerization and transalkylation of the ring-alkylated products is likely to occur under these conditions.[7,33]

Figure 1b shows the evolution of the alkylation products as a function of reaction time. Initially, the two primary alkylation products, IMP and MIPB, were formed at similar rates, but soon they were consumed to make secondary products. It is important to note that the O-alkylated products (MIPB) undergo a much faster decay compared to the ring-alkylated products. This observation is in agreement with previous reports indicating that selectivity to ethers decreases with reaction time (or space time in flow systems).[12,34] As discussed below, this is due to the fast ether decomposition rate in the presence of an acid catalyst. As a result, it is observed that after 2 h of reaction, DIMP became the dominant product, with a smaller concentration of IMIPB. The concentration of TIMP and DIMIPB was always minor as compared to the other products. It is also worth noting the change in the conversion rate of m-cresol, which reached a plateau with reaction time, even before the reactant was consumed, or reaching equilibrium. Therefore, in a batch reactor, this is an indication of catalyst deactivation, and as presented below, catalyst deactivation needs to be incorporated in the analysis when developing the kinetic model.

Verification of the absence of mass transfer limitations

Before further experimentation or data analysis, it was important to probe the system and rule out mass or heat transfer limitations. The Koros–Nowak criterion states that the rate of reaction is directly proportional to the concentration of active sites in a catalyst. However, when the reaction is influenced by external or internal mass transfer or heat transfer limitations the rate will not be directly proportional to the concentration of active sites. Koros and Nowak[35] used their test by mixing two powders, one inert and the other is catalytic, at varying ratios, thus, creating a series of samples with different active sites concentration. If the reaction rate, after being normalized to the concentration of active sites, does not change for the different catalysts then the system is exempt from transport limitations. In a similar test, Madon and Boudart[30] compared a series of supported metal catalysts with varying metal loading. This test, proposed more than 30 years ago, has been used successfully in many studies on

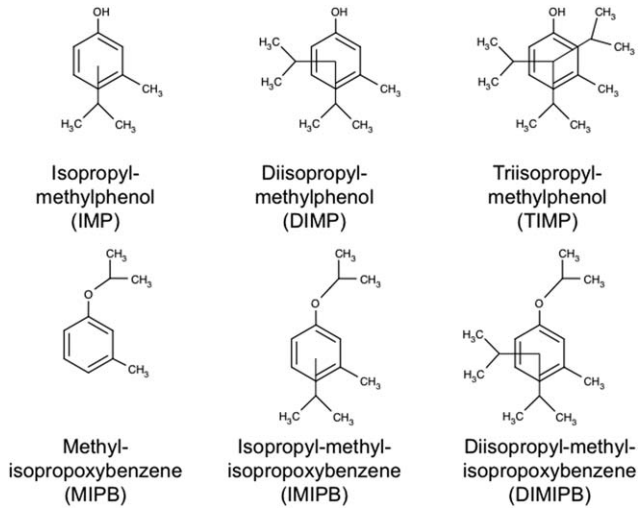

Scheme 1. Products from alkylation of m-cresol with isopropanol.

Table 1. Acid Site Density of Zeolites Used for Mass Transport Limitations Test: Original Zeolite Was an HY with Si/Al = 30 (First Row)

Sodium Used for Exchange (μmol/g zeolite)	Theoretical Brønsted Acid Site Density (μmol/g zeolite)	Measured Brønsted Acid Site Density (μmol/g zeolite)
0	538	248
67	471	218
100	438	190

supported metal catalysts. However, the criterion has been much less common in studies of acidic zeolites.[36] In this work, we varied the concentration of acid sites of a HY zeolite (Si/Al = 30) by ion exchange with sodium hydroxide and used the resulting catalysts to determine whether the alkylation reaction was transport limited.

Three zeolites were obtained and their Brønsted acidity is reported in Table 1. It is clear that the measured concentration of acid sites was lower than the expected value. To achieve the Si/Al ratio of the zeolite used in this study, this material had to undergo a dealumination process during manufacturing, which includes steaming and acid leaching. During this process, most of the Al is removed from the tetrahedral positions in the framework, forming octahedral extra-framework species. Although the steamed zeolite is acid treated to remove some of the extra-framework Al, a large fraction still remains in the solid as octahedral Al. In fact, nuclear magnetic resonance (NMR) characterization of HY Si/Al = 30 revealed the presence of both of these aluminum species, which is usually accompanied by a significant presence of mesopores, also generated from the dealumination process (see Supporting Information, Figures S1, S2, and Table S1). Of course, extra-framework Al still counts toward the atomic Si/Al ratio of the zeolite. However, it does not contribute to the number of acid sites present in the catalyst. Therefore, it was expected that the measured acid site density was lower than the theoretical value for a given Si/Al ratio.

About 50% of the Brønsted acid sites were exchanged, and a significant difference in acid site concentration between the samples was obtained. Figure 2 shows the specific reaction rate (Turnover Frequency - TOF) for the alkylation of m-cresol on a per site basis with the various exchanged zeolites. The values are equivalent within the experimental error and certainly do not decrease as a function of acid site density, which would be expected if mass transfer limitations were present. To avoid the effects of any catalyst deactivation, the values reported correspond to short reaction times, as deactivation could depend on density of acid sites and mask the true TOF.

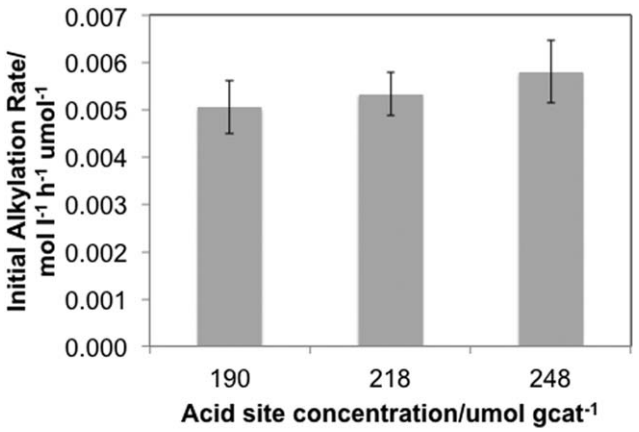

Figure 2. Initial alkylation rates for catalysts with different acid site concentration.

Conditions: IPA/m-cresol = 3.8, T = 473 K, P = 4.8 MPa, reaction time: 1 h.

Alkylation of isopropyl-methylphenol (thymol) and IPB decomposition

The observed product distribution reveals the complexity of the alkylation reaction system in terms of the number of different steps that possibly take place. It is clear that to get a better understanding of the reaction pathways and generate a reliable kinetic model additional experimental data are required. Accordingly, the alkylation of one of the isomers of the IMP, thymol, with isopropanol was carried out under the same conditions as those used for m-cresol alkylation. As shown in Figure 3a, dehydration of isopropanol to diisopropyl ether and propylene readily occurred, as in the case of m-cresol alkylation. Conversely, DIMP was the dominant alkylation product, while MIPB and trialkylated products (TIMP and DIMIPB) only appeared in low concentrations. A similar deactivation pattern to that observed during m-cresol alkylation was evident as the rate of IMP (thymol) consumption leveled off after 4 h of reaction, despite the presence of a significant amount of unconverted IMP.

In a separate set of experiments, the decomposition of IPB was studied in the presence of HY zeolite. Methylisopropoxybenzene (MIPB; Scheme 1), is not available commercially, but its analog IPB provided valid information regarding the reactivity of the ether functionality, which has been a subject of interest in previous studies reported in the

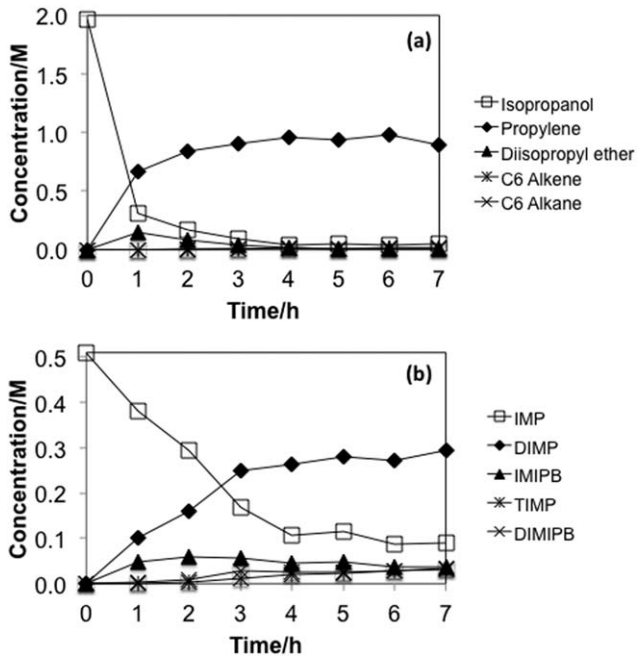

Figure 3. Product distribution from alkylation of thymol (akylated) with isopropanol.

(a) Dehydration/oligomerization products. (b) Alkylation products. Conditions: isopropanol/thymol = 3.8, T = 473 K, P = 4.8 MPa, catalyst mass = 50 mg HY.

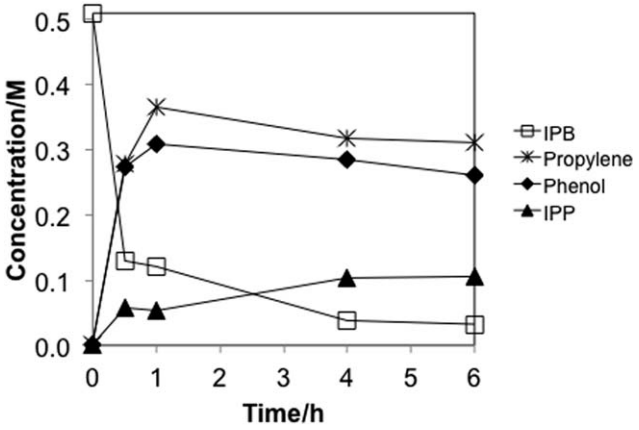

Figure 4. Product distribution from decomposition of IPB.

Conditions: initial concentration = 0.51 M, $T = 473$ K, $P = 4.8$ MPa, catalyst mass = 50 mg HY.

literature. For example, in a study on the alkylation of phenol with methanol,[33] it was proposed that anisole (i.e., the ether product) reacts with phenol to give cresol and phenol, suggesting a bimolecular mechanism for interconversion of ether- to ring-alkylated products. Alternatively, computational studies about the alkylation of phenol with *tert*-butanol indicate that the ether product undergoes an intramolecular rearrangement, leading to a direct transformation into a ring-alkylated product.[34,37]

Figure 4 shows the product distribution from IPB ether decomposition (i.e., no isopropanol added) as a function of reaction time. It is clear that phenol and propylene were the primary products from a fast cleavage of the ether bond. Thus, the proposed intramolecular rearrangement mechanism is not supported by our experiments. Rather, as depicted in Scheme 2, the ring-alkylated product isopropylphenol (IPP) is a secondary product that arises from the alkylation of phenol with propylene, both resulting from the initial ether decomposition.

Effect of alkylating agent

Alkylation of phenolic compounds is an electrophilic substitution reaction, in which an electron-enriched group in the phenolic molecule attacks an electrophile. There are two electron-enriched groups in m-cresol that could perform an electrophilic attack: the aromatic ring and the oxygen atom in the hydroxyl group. They are able to yield C-alkylation products and O-alkylation products, respectively. The oxygen atom in the hydroxyl group has a higher electron density in the highest occupied molecular orbital as compared to the carbon atoms in ortho and para positions, making

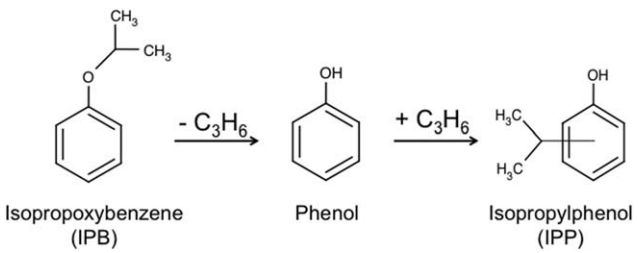

Scheme 2. IPB decomposition and subsequent alkylation.

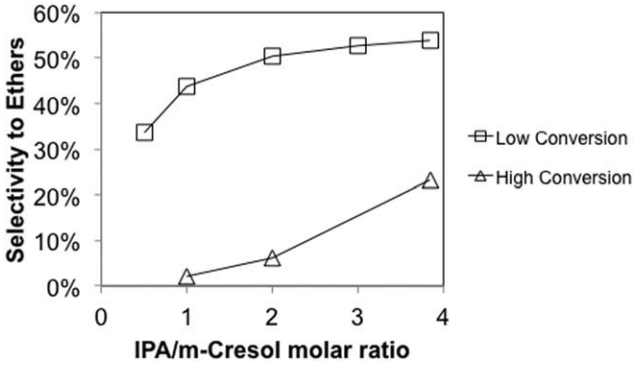

Figure 5. Effect of isopropanol/m-cresol molar ratio and conversion on the selectivity to etherification products.

O-alkylation favored over C-alkylation, at least initially.[37] Regarding the electrophile (alkylating agent), there are also two possibilities. In the presence of an acid, isopropanol can undergo protonation and generate an oxonium species. Also, on dehydration of this oxonium ion, a carbenium ion is formed on the surface, which after desorption produces an olefin. At the same time, an olefin from the bulk phase can readsorb and form again a carbenium ion. Due to the high concentration of propylene observed in the reactor, it can be assumed that the main source of carbenium ion formation is the protonation of propylene rather than the dehydration of an oxonium ion. Both of these ionic species (oxonium and carbenium ions) would be able to undergo an electrophilic attack. From our initial experiments, it is not clear whether isopropanol or propylene is the alkylating agent for C- and O-alkylation, or if the two of them play a similar role in both alkylation reactions.

To clarify the role of the alkylating agent, we performed a series of experiments with different concentrations of isopropanol and propylene and compared the selectivity toward C-alkylated (IMP, DIMP, TIMP) and O-alkylated (MIPB, IMIPB, DIMIPB) products. Figure 5 shows the variation of selectivity toward ethers with the isopropanol/m-cresol molar ratio in the feed. The comparison was done at two levels of conversion, low (11–17%) and high (56–62%). It is clear that the selectivity to ethers is significantly higher at lower conversion. The drastic decrease in the overall ether selectivity at high conversion is most likely due to the fast ether decomposition mentioned above. However, for a given conversion level, this selectivity increases with the isopropanol/m-cresol ratio, in agreement with the trends reported for the alkylation of m-cresol and o-cresol with isopropanol[12,38] and *tert*-butanol.[34] As shown in Figure 6, using propylene as alkylating agent instead of isopropanol, at the same C3/m-cresol ratio and same level of conversion, results in a much lower selectivity toward ethers. Therefore, while the carbenium ion forming from the olefin is able to alkylate both the oxygen and the carbon atoms in m-cresol, the use of isopropanol as alkylating agent favors the formation of the ether as primary product.

From our previous studies,[7] conducted in the vapor phase, one would have not predicted this difference. In fact, we showed that isopropanol dehydration is much faster than the m-cresol alkylation reaction and as a result, propylene would be the alkylating agent, essentially erasing any differences in the subsequent alkylation. Likewise, as shown in Figures 1

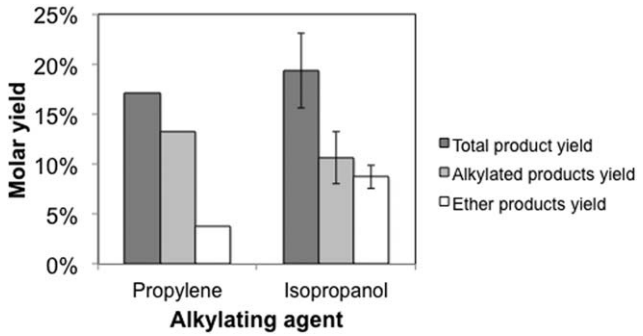

Figure 6. Alkylated and ether product yields for alkylation of m-cresol with propylene and isopropanol.

Conditions: isopropanol or propylene/m-cresol = 3.8, $T = 473$ K, $P = 4.8$ MPa, catalyst mass = 20 mg HY, reaction time = 1 h.

and 4, dehydration is also faster than alkylation in the liquid phase, enhancing the possibility that the oxonium ion quickly dehydrates and forms an olefin on the surface before it can start the alkylation step. In that case, the protonated olefin would be responsible for both O- and C-alkylation, while isopropanol would only be the precursor for the alkylating agent.

To shed light to this conundrum, alkylation of m-cresol was performed with *n*-propanol. Protonation of this alcohol should form a primary oxonium ion, which on dehydration would form a secondary carbenium ion, because of its higher stability over a primary carbenium ion. Alkylation from a secondary carbenium ion would in turn lead to isopropyl-alkylated phenols. However, if the primary oxonium ion serves as the alkylating agent, then *n*-propyl-alkylated phenols should be observed. In fact, as shown in Figure 7, both *n*-propyl-alkylated ring and *n*-propyl ethers are the main reaction products of the alkylation with *n*-propanol, leading to the conclusion that the oxonium ion formed by protonation of the alcohol is able to undergo electrophilic attack by both the aromatic ring and the oxygen of the hydroxyl group in m-cresol. However, it should be noted that *n*-propanol is significantly slower than dehydration of isopropanol. This is evident by the significantly lower yield of alkylation products obtained with the former (i.e., comparing Figures 6 and 7). One could argue that, due to the slower dehydration of *n*-propanol, the oxonium ion has more time to act as direct alkylating agent, whereas in the case of isopropanol dehydration is fast and the presence of oxonium ions is limited. Nevertheless, taking all the results together, we conclude that, even if it less important than the carbenium ion, the oxonium ion is also a direct alkylating agent. Also, both O- and C-alkylation can take place with both ionic species, oxonium and carbenium. This conclusion is in agreement with recent computational studies of the alkylation of phenolics with *tert*-butanol, which show that the energy barriers for alkylation with the alcohol and the respective olefin are not significantly different.[39]

Reaction pathways and kinetic model

Based on this qualitative analysis of the experimental results, we have proposed a reaction scheme for alkylation of m-cresol with isopropanol in a HY zeolite (Scheme 3) that forms the basis of a more quantitative kinetic model. Accordingly, the first step is the dehydration of the alcohol. From our experiments and previous studies, it was observed that dehydration of isopropanol can occur via two parallel paths, one is the direct dehydration and the other via formation of di-isopropyl ether, which can further decompose to propylene and water.[38]

$$\text{Isopropanol} \rightarrow \text{Propylene} + \text{Water} \quad (1)$$

$$\text{Isopropanol} \rightarrow \text{Di}-\text{isopropyl ether} + \text{Water} \quad (2)$$

$$\text{Di}-\text{isopropyl ether} \rightarrow \text{Propylene} + \text{Water} \quad (3)$$

To reduce the number of parameters in the model, and taking into account the fast rate of di-isopropyl ether decomposition, these three reactions were simplified into step (1). To consider the potential role of the reverse reaction, the equilibrium constant at 473 K was calculated ($K_{EQ} = 2508$) and used to relate the forward reaction with the reverse reaction.

$$k_{d-1} = k_{d1}/K_{EQ} \quad (4)$$

According to the previous discussion, the alkylation of m-cresol was considered to occur by the O- and C-alkylation routes, involving both, isopropanol and propylene as alkylating agents. The ether products can undergo decomposition to form propylene and the correspondent phenolic or subsequent C-alkylation with either isopropanol of propylene. In parallel, ring-alkylated products participate in the same type of reactions as m-cresol. It is important to note that, based on our experimental results, intramolecular arrangement (isomerization) of ethers is not considered. Additionally, a zero-order polymerization reaction leading to insoluble products was included in the model. This path showed a low rate compared to other relevant reactions, as the mole balance for most reactions was above 90%. However, it allowed us to completely close the mass balance and account for all the species formed during reaction.

The two conventional Langmuir–Hinshelwood and Eley–Rideal models were used to analyze the reaction scheme. In both cases, the participation of reactants, products, and solvent in competitive adsorption on the catalyst surface was considered. For Langmuir–Hinshelwood, the rate-limiting step was the reaction between two adsorbed species (phenolic and alkylating agent), except in the case of ether

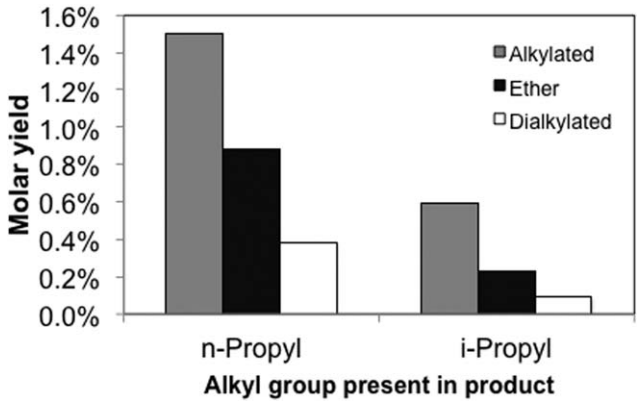

Figure 7. Product yields for alkylation of m-cresol with *n*-propanol.

Conditions: *n*-propanol/m-cresol = 3.7, $T = 473$ K, $P = 4.8$ MPa, catalyst mass = 50 mg HY, reaction time = 1 h.

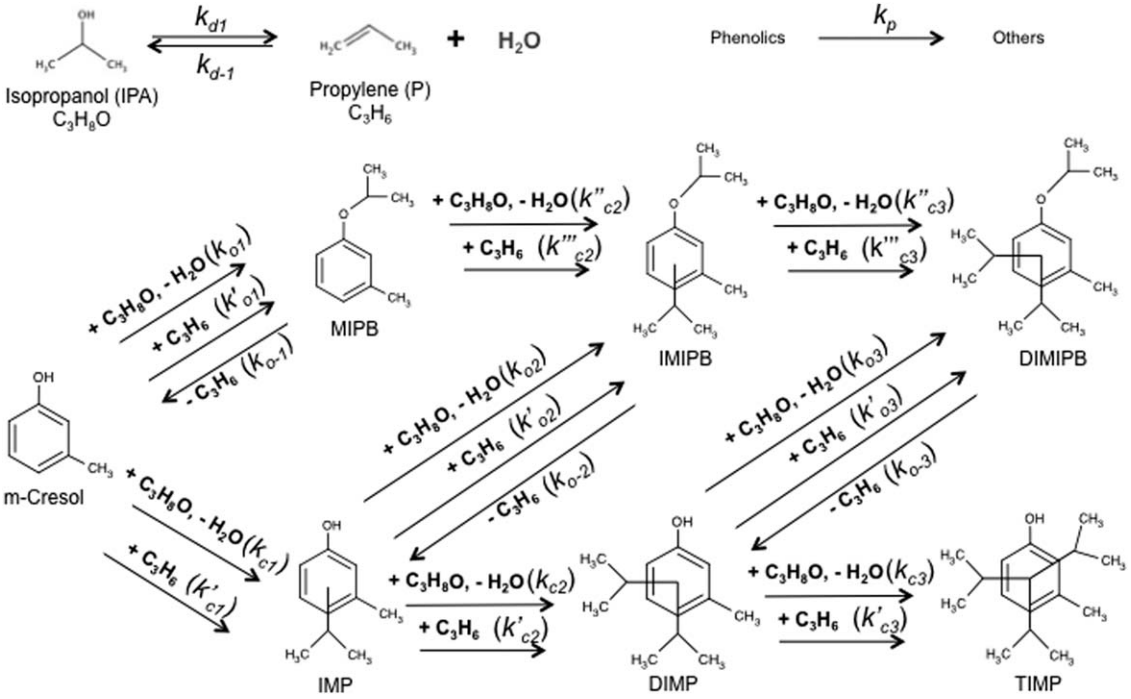

Scheme 3. Reaction scheme for the reaction of m-cresol with isopropanol in the presence of HY zeolite.

C_3H_8O : Isopropanol. C_3H_6 : Propylene.

decomposition and alcohol dehydration, where the rate was only proportional to the surface concentration of a single reactant. As an example, the coverage and mole balance for isopropanol are shown below.

$$\theta_{IPA}=[K_{IPA}C_{IPA}]/[1+K_{IPA}C_{IPA}+K_PC_P+K_{H_2O}C_{H_2O}+K_CC_C+K_{PHEN}(C_{IMP}+C_{DIMP}+C_{TIMP})+K_{ETHER}(C_{MIPB}+C_{IMIPB}+C_{DIMIPB})] \quad (5)$$

$$dC_{IPA}/dt=[-k_{d1}\theta_{IPA}+k_{d\text{-}1}\theta_P\theta_{H_2O}-k_{o1}\theta_{IPA}\theta_C-k_{o2}\theta_{IPA}\theta_{IMP}-k_{o3}\theta_{IPA}\theta_{DIMP}-k_{c1}\theta_{IPA}\theta_C-k_{c2}\theta_{IPA}\theta_{IMP}-k_{c3}\theta_{IPA}\theta_{DIMP}-k''_{c2}\theta_{IPA}\theta_{MIPB}-k''_{c3}\theta_{IPA}\theta_{IMIPB}] \quad (6)$$

For simplicity, a general adsorption constant K_{PHEN} was defined for ring-alkylated products (IMP, DIMP, TIMP) and K_{ETHER} for ether products (MIPB, IMIPB, DIMIPB). Conversely, for the Eley–Rideal model, the rate-limiting step for alkylation was the reaction between an adsorbed molecule of alkylating agent and a nonadsorbed phenolic molecule (m-cresol, ring-alkylated, or ether). Again, an example of the mole balance for isopropanol is shown below.

$$dC_{IPA}/dt=[-k_{d1}\theta_{IPA}+k_{d\text{-}1}\theta_P\theta_{H_2O}-k_{o1}\theta_{IPA}C_C-k_{o2}\theta_{IPA}C_{IMP}-k_{o3}\theta_{IPA}C_{DIMP}-k_{c1}\theta_{IPA}C_C-k_{c2}\theta_{IPA}C_{IMP}-k_{c3}\theta_{IPA}C_{DIMP}-k''_{c2}\theta_{IPA}C_{MIPB}-k''_{c3}\theta_{IPA}C_{IMIPB}] \quad (7)$$

The concentration of propylene was modeled using an estimate of the Henry's constant under the reaction conditions.[40] Propylene partial pressure was estimated from the moles of propylene in the system and the ideal gas equation. As Henry's constant relates the partial pressure to the liquid composition, the liquid concentration of propylene was calculated from the following equation.

$$C_P=(p_P * \rho_{Solv})/H_P^{473K} \quad (8)$$

Finally, as mentioned above, the catalyst undergoes significant deactivation under the reaction conditions. Decay in activity could be due to oligomerization of propylene that promotes coke formation,[41] strong adsorption of phenolic compounds,[13] or zeolite degradation due to the presence of liquid water.[6,10] Previous studies have described the deactivation of zeolites in terms of an activity function, defined in terms of the deactivation mechanism, either pore plugging or active sites fouling.[42,43] This deactivation function has two adjustable parameters and it was coupled with our kinetic model by combining it with each mole balance. Also for isopropanol, the resultant equation is shown below. As expected, the rate of reaction decreases as a function of time when this function is used.

$$dC_{IPA}/dt=[-k_{d1}\theta_{IPA}+k_{d\text{-}1}\theta_P\theta_{H_2O}-k_{o1}\theta_{IPA}\theta_C-k_{o2}\theta_{IPA}\theta_{IMP}-k_{o3}\theta_{IPA}\theta_{DIMP}-k_{c1}\theta_{IPA}\theta_C-k_{c2}\theta_{IPA}\theta_{IMP}-k_{c3}\theta_{IPA}\theta_{DIMP}-k''_{c2}\theta_{IPA}\theta_{MIPB}-k''_{c3}\theta_{IPA}\theta_{IMIPB}][(B+1)/(B+e^{At})] \quad (9)$$

A mole balance in the form of Eq. 9 was established for every species observed in the reaction (see Scheme 3). With initial estimates for the model parameters (rate, adsorption, and deactivation constants), the mole balance equations allowed to estimate the concentration profile for each individual species. Finally, using a least squares method, the model parameters were adjusted to provide the best possible fit to the experimental data within the given constrains (described in the next section). Therefore, the measured concentration of each species as a function of time was used in

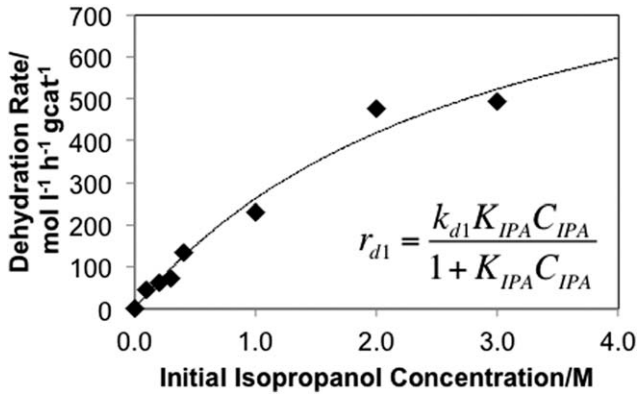

Figure 8. Rate of isopropanol dehydration measured at different isopropanol concentrations and short reaction time.

Conditions: $T = 473$ K, $P = 4.8$ MPa, catalyst mass = 10 mg HY, reaction time = 0.2 h.

the kinetic model, including all the data contained in Figures 1 and 3. The model results for the case where m-cresol was used as the feed are shown in Figures S3 and S4.

Validating model by independent rate measurements and added constrains

Due to the complexity of the several phenomena involved, the resulting reaction scheme generates a large number of adjustable variables (rate constants, adsorption constants, and deactivation parameters) for the kinetic model. Therefore, to provide independent measurements, reduce the level of uncertainty, and improve the precision of the fitting results we performed two additional sets of experiments with individual reactants, dehydration of isopropanol, and decomposition of IPB. Both reactions are simpler than the alkylation reaction, require only one reactant, and play a crucial role in the overall reaction scheme. They were performed individually to estimate rate constants for dehydration and ether decomposition that were then used as initial guesses and to define limits for these variables in the kinetic model.

Next, reaction measurements were conducted in differential mode (low conversion) to eliminate the influence of

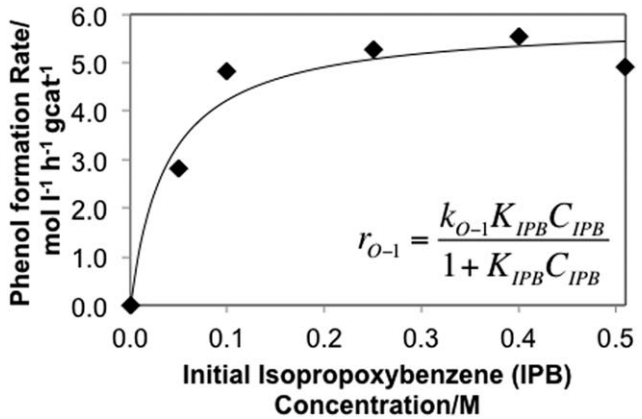

Figure 9. Rate of IPB decomposition measured at different IPB concentrations and short reaction time.

Conditions: $T = 473$ K, $P = 4.8$ MPa, catalyst mass = 20 mg HY, reaction time = 0.5 h.

Table 2. Adsorption Constants of Reactants and Products on HY Zeolite in the Reaction of m-Cresol with Isopropanol Using Two Different Kinetic Models: Units Are [L mol^{-1}]

	Adsorption Constant	
Compound	Langmuir–Hinshelwood	Eley–Rideal
Isopropyl alcohol	1.0	1.0
Propylene	10	10
Water	10	10
Cresol	20	21
Ring-alkylated products	61	63
Ether products	41	42
Decalin	0	0

products in the rate expression, and thus, obtaining kinetic constants with less adjustable parameters. That is, the rate of reaction for dehydration of isopropanol as stated in Eq. 3 can be written based on a Langmuir–Hinshelwood mechanism as follows

$$r_{d1} = [k_{d1} K_{IPA} C_{IPA}] / [1 + K_{IPA} C_{IPA} + K_P C_P + K_{H_2O} C_{H_2O}] \quad (10)$$

At low conversion, this expression can be simplified as

$$r_{d1} = [k_{d1} K_{IPA} C_{IPA}] / [1 + K_{IPA} C_{IPA}] \quad (11)$$

Equation 11 was used to fit the data in Figure 8 for isopropanol dehydration at low conversions. The resulting rate of dehydration was 1040 [mol L^{-1} h^{-1} gcat^{-1}] and the adsorption constant 0.34 (L mol^{-1}). In the same way, the rate of decomposition of IPB (an analog of MIPB) at low conversions can be written based on a Langmuir–Hinshelwood mechanism

$$r_{d1} = [k_{o-1} K_{IPB} C_{IPB}] / [1 + K_{IPB} C_{IPB}] \quad (12)$$

Data from Figure 9 was fitted using Eq. 12. A rate constant of 5.9 [mol L^{-1} h^{-1} gcat^{-1}] and an adsorption constant of 26 (L mol^{-1}) were obtained.

Moreover, further constraints were set on the model based on general knowledge and experimental observations obtained from previous studies. The constraints used for the kinetic fitting of both Langmuir–Hinshelwood and Eley–Rideal models are listed below.

1. Isopropanol dehydration
   a. Rate constant initial guess (k_{d1}): 1040 [mol L^{-1} h^{-1} gcat^{-1}]. From experiments (Figure 8).
   b. Rate constant limits: $k_{d1} < 1240$ [mol L^{-1} h^{-1} gcat^{-1}]. Allows k_{d1} to increase up to 20% of the initial guess.
   c. Adsorption constant initial guess (K_{IPA}): 0.34 (L mol^{-1}). From experiments (Figure 8).
   d. Adsorption constant limits: $K_{IPA} < 1$ (L mol^{-1}). Allows K_{IPA} to increase without changing its order of magnitude.

Table 3. Rate Constants for Dehydration and Polymerization in the Reaction of m-Cresol with Isopropanol Using Two Different Kinetic Models: Units Are [mol L^{-1} h^{-1} gcat^{-1}]

	Rate Constant	
Reaction	Langmuir–Hinshelwood	Eley–Rideal
Dehydration (forward) k_{d1}	1240	1240
Dehydration (reverse) k_{d-1}	16	16
Polymerization k_p	0.17	0.15

Table 4. Rate Constants for Alkylation and Ether Decomposition in the Reaction of m-Cresol with Isopropanol Using a Langmuir-Hinshelwood Kinetic Model: Units Are [mol L^{-1} h^{-1} $gcat^{-1}$]

	C-Alkylation		O-Alkylation		Ether Decomposition
Phenolic\Alkylating agent	Isopropanol	Propylene	Isopropanol	Propylene	None
m-Cresol	k_{c1}	k'_{c1}	k_{o1}	k'_{o1}	
	80	80	88	44	
IMP	k_{c2}	k'_{c2}	k_{o2}	k'_{o2}	
	20	41	30	15	
DIMP	k_{c3}	k'_{c3}	k_{o3}	k'_{o3}	
	4	4	1	1	
MIPB	k''_{c2}	k'''_{c2}			k_{o-1}
	33	66			7
IMIPB	k''_{c3}	k'''_{c3}			k_{o-2}
	22	44			7
DIMIPB					k_{o-3}
					7

2. Ether decomposition
   a. Rate constant initial guess (k_{o-1}, k_{o-2}, k_{o-3}): 5.9 [mol L^{-1} h^{-1} $gcat^{-1}$]. From experiments (Figure 9).
   b. Rate constant limits: $4.7 < k_{o-1}, k_{o-2}, k_{o-3} < 7.1$ [mol L^{-1} h^{-1} $gcat^{-1}$]. Allows ko's to vary within ±20% of initial guess.
   c. Adsorption constant initial guess (K_{ETH}): 26 (L mol^{-1}). From experiments (Figure 9).
3. Deactivation parameters
   a. Limits: $A,B < 20$. Limits parameters to the range reported in the literature.[42,43]
4. Adsorption constants
   a. Ethers adsorption constant initial guess: 26 (L mol^{-1}). From experiments (Figure 9).
   b. m-Cresol and phenolics adsorption constant limits: $(0.5*K_{ETH}) < K_C$, $K_{PHEN} < (1.5*K_{ETH})$. Limits K_C and K_{PHEN} to the same range of K_{ETH}.
   c. Propylene adsorption constant: $(0.5*K_C) < K_P < (1.5*K_C)$. Limits K_P to the same range of K_C.
   d. Water adsorption constant: $K_{H_2O} \geq K_P$. Keeps K_{H_2O} in the same range as that of hydrocarbons and phenolics.[44]
5. Alkylation.
   a. Rate constants for O-alkylation with isopropanol were higher than the respective reaction with propylene. From experiments (Figure 6).
   b. Rate constants for C-alkylation with propylene were higher than the respective reaction with isopropanol. From experiments (Figure 6).

Kinetic modeling results

From the fitting of the experimental data with the constraints described above, we have obtained thermodynamic and kinetic parameters with physical significance. For example, as shown in Table 2, adsorption constants were obtained for all the species present on the surface. Similarly, Tables 3–5 summarize rate constants for all reactions, while Table 6 includes the resulting parameters for the deactivation function. Table 2 shows the resultant adsorption constants for both Langmuir–Hinshelwood and Eley–Rideal models. No difference was observed in the values obtained from these models. Adsorption of propylene and water was significantly stronger than that of isopropanol, evident by an order of magnitude difference in adsorption constants. The group adsorption constant for phenolic compounds K_{PHEN} was significantly higher than the adsorption constant for m-cresol. Phenolic compounds can take different configurations when adsorbing on acidic catalysts.[29,41,45] If the aromatic ring interacts in a parallel geometry with the surface, an increase in the number of alkyl substituents might enhance the adsorbate–surface interaction.[46] Also, increasing the number of alkyl substituents can result in enhanced adsorption entropy with a corresponding increase in the observed adsorption constant for the ring-alkylated products compared to m-cresol.

The adsorption constant for the ether lies somewhere between those of m-cresol and phenolics. Its interaction with the surface is likely to take place through the oxygen atom

Table 5. Rate Constants for Alkylation and Ether Decomposition in the Reaction of m-Cresol with Isopropanol Using an Eley-Rideal Kinetic Model: Units Are [$(h*g\ cat)^{-1}$] for Alkylation and [mol L^{-1} h^{-1} $gcat^{-1}$] for Ether Decomposition

	C-Alkylation		O-Alkylation		Ether Decomposition
	Isopropanol	Propylene	Isopropanol	Propylene	None
m-Cresol	k_{c1}	k'_{c1}	k_{o1}	k'_{o1}	
	41	**41**	**37**	**19**	
IMP	k_{c2}	k'_{c2}	k_{o2}	k'_{o2}	
	27	**54**	**31**	**15**	
DIMP	k_{c3}	k'_{c3}	k_{o3}	k'_{o3}	
	4	**4**	**12**	**6**	
MIPB	k''_{c2}	k'''_{c2}			k_{o-1}
	27	**27**			**7**
IMIPB	k''_{c3}	k'''_{c3}			k_{o-2}
	3	**5**			**7**
DIMIPB					k_{o-3}
					7

Table 6. Deactivation Parameters in the Reaction of m-Cresol with Isopropanol

	Deactivation Parameters
A (h^{-1})	0.32
B	20

in the hydroxyl group, leading to the fast carbon–oxygen bond cleavage observed experimentally. Finally, decalin appeared to have a rather weak interaction with the surface, as compared to the reactants and products, as reflected in a low adsorption constant.

Rate constants for dehydration and polymerization are shown in Table 3. As in the previous case, there is not significant difference in the results from Langmuir–Hinshelwood and Eley–Rideal kinetic models. Table 4 shows the rate constants obtained from the Langmuir–Hinshelwood model for the multiple alkylation steps and both C- and O-alkylation. A clear trend is observed; the bulkier is the molecule being alkylated, the slower is the alkylation rate. For C-alkylation with isopropanol, the order in rate constant is as follows: $k_{c1} > k_{c2} > k_{c3}$ and $k''_{c2} > k''_{c3}$, and the same trend is true for C-alkylation with propylene and for O-alkylation. In principle, the addition of an alkyl group to the aromatic ring should increase its electron density, thus, generating a higher probability for an electrophilic attack. However, steric constraints start to be important as the number of substituents in the phenolic molecule increases, leading to a limitation in the alkylation rate. These constraints could originate from the molecule itself, that is, the high substitution of the ring could hinder the addition of an alkyl group, or from the porous character of the catalyst, that is, the pores are not big enough to hold the product. The later under the assumption that most active sites are inside the pores and the external surface does not play an important role in catalytic activity. As a matter of fact, it has been suggested that the pore size of zeolites could limit consecutive alkylation due to geometric constraints,[7] and even some authors have used this limitation as a tool for controlling product selectivity in alkylation reactions.[33]

C-alkylation and O-alkylation happened at similar rates for m-cresol and IMP, whereas they showed a more pronounced difference for DIMP. A comparison of the

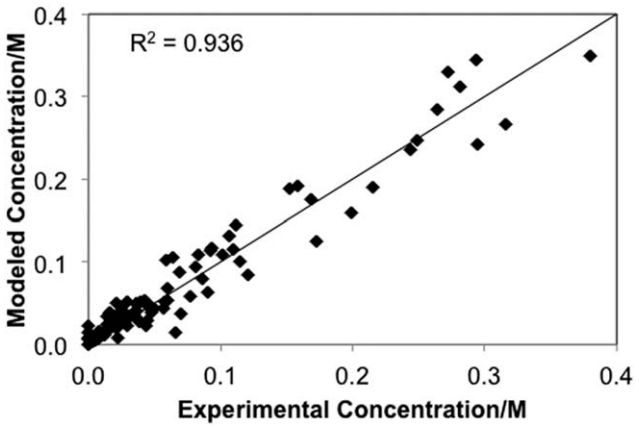

Figure 10. Langmuir-Hinshelwood kinetic model results.

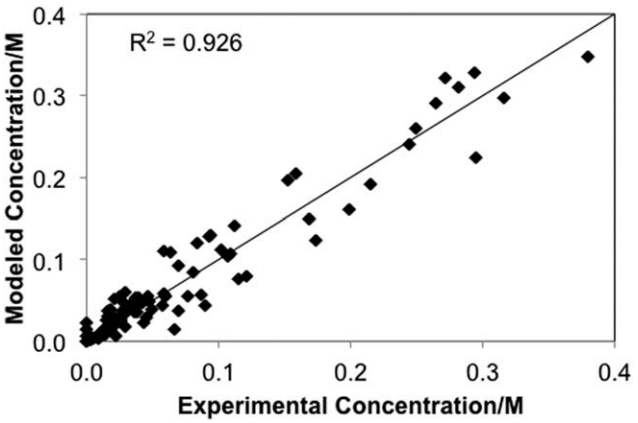

Figure 11. Eley-Rideal kinetic model results.

C-alkylation of IMP vs. MIPB reveals a faster rate constant for the ether. MIPB has only two substituents in the ring, a methyl and an isopropoxy group, whereas IMP has three ring substituents. Electronically, IMP should be more active for ring alkylation than the ether, as suggested by previous results from alkylation of phenol with methanol.[13] However, a methyl group is not as bulky as an isopropyl group and is possible the later could introduce important geometric constraints. Therefore, one could expect for MIPB to undergo a faster alkylation due to lower steric limitations as compared to IMP. Another interesting result is found when comparing the rate constants for C-alkylation of m-cresol vs. MIPB. Even though these two compounds have the same number of substituents in the ring, alkylation takes place faster in m-cresol. The presence of the bulky isopropyl group in the ether can indeed hinder alkylation at the ortho position, which would be the preferred substitution otherwise. As a consequence the overall rate of alkylation is lower for MIPB. Similar trends were observed for the Eley–Rideal kinetic model, although they are not as consistent with the expected trends as in the case of the Langmuir–Hinshelwood model. As shown in Table 5, for this model the difference between alkylation of m-cresol and IMP was not as pronounced as predicted from the Langmuir–Hinshelwood model, but their rate constants are in roughly the same order. It is possible that phenolic molecules in the bulk phase have geometrically more freedom to interact with the alkylating agent than if they were adsorbed, therefore, lifting some of the steric constraints implied by the Langmuir–Hinshelwood model. Overall, both models offered a good fitting as depicted in Figures 10 and 11.

Water produced from dehydration is present in significant amounts, even to the point of creating a new phase in the reaction mixture. However, the role it plays in activity is not clear yet. Some authors have highlighted the positive effects of water in reaction rates when using zeolites, either by inhibiting olefin oligomerization or generating additional acid sites.[7,47] Conversely, hot liquid water can significantly degrade the zeolite crystalline structure, and thus, negatively impact activity.[6,10] In light of these observations, further studies are required to elucidate the role of water in zeolite deactivation during m-cresol alkylation.

The deactivation function provides a good representation of the variation of activity with time, but does not allow us to establish a deactivation mechanism from the estimated

deactivation parameters, mainly because there are many additional factors in play, as described above.

Conclusions

Alkylation of m-cresol with short oxygenates in the liquid phase is an important reaction in the conversion of biomass for production of fuels and chemicals. This study focuses on the understanding of the alkylation of m-cresol with isopropanol reaction in the liquid phase on a HY zeolite. To gain insight about the reaction pathways, experimental data have been obtained and fitted using two kinetic models, Langmuir–Hinshelwood and Eley–Rideal. Products from C- and O-alkylation were observed followed by multiple alkylation products. C-alkylation was found to be favored in the presence of propylene, whereas O-alkylation was enhanced when isopropanol concentration increased. Propylene also alkylates phenolics via both, C- and O-alkylation. The O-alkylation product IPB rapidly decomposes into propylene and phenol, which could further undergo alkylation. This is contrary to the hypothesis of intramolecular arrangement (isomerization) of ethers into ring-alkylated products previously proposed in the literature. Fitting of the experimental data with the kinetic models allowed the estimation of adsorption and rate constants according to the proposed reaction pathway. Both models offered a similar quality in the fitting, and showed similar trends in the resultant kinetic and adsorption parameters. In general, the rate of alkylation decreased with the number of alkyl substituents in the phenolic molecule, most likely due to steric constraints that limit the entrance of an additional alkyl group.

Acknowledgments

This work was supported by the U.S. Department of Energy, EPSCOR, under Award # DE-SC0004600.

Literature Cited

1. Alonso DM, Bond JQ, Dumesic JA. Catalytic conversion of biomass to biofuels. *Green Chem.* 2010;12:1493–1513.
2. Tong X, Ma Y, Li Y. Biomass into chemicals: conversion of sugars to furan derivatives by catalytic processes. *Appl Catal A.* 2010;385: 1–13.
3. Goyal HB, Seal D, Saxena RC. Bio-fuel from thermochemical conversion of renewable resources: a review. *Renew Sustain Energy Rev.* 2008;12:504–517.
4. Qi Z, Jie C, Tiejun W, Ying X. Review of biomass pyrolysis oil properties and upgrading research. *Energy Convers Manag.* 2007;48: 87–92.
5. Mohan D, Pittman CU, Steele PH. Pyrolysis of wood/biomass for bio-oil: a critical review. *Energy Fuels.* 2006;20:848–889.
6. Zapata PA, Huang Y, González-Borja MA, Resasco DE. Silylated hydrophobic zeolites with enhanced tolerance to hot liquid water. *J Catal.* 2013;308:82–97.
7. Nie L, Resasco DE. Improving carbon retention in biomass conversion by alkylation of phenolics with small oxygenates. *Appl Catal A.* 2012;447–448:14–21.
8. Pham TN, Sooknoi T, Crossley S, Resasco DE. Ketonization of carboxylic acids: mechanisms, catalysts, and implications for biomass conversion. *ACS Catal.* 2013;3:2456–2473.
9. Pham TN, Shi D, Sooknoi T, Resasco DE. Aqueous-phase ketonization of acetic acid over Ru/TiO_2/carbon catalysts. *J Catal.* 2012;295: 169–178.
10. Zapata PA, Faria J, Ruiz MP, Jentoft RE, Resasco DE. Hydrophobic zeolites for biofuel upgrading reactions at the liquid-liquid interface in water/oil emulsions. *J Am Chem Soc.* 2012;134:8570–8578.
11. Grabowska H, Syper L, Zawadzki M. Vapor phase alkylation of *ortho*-, *meta*- and *para*-cresols with isopropyl alcohol in the presence of sol-gel prepared alumina catalyst. *Appl Catal A.* 2004;277:91–97.
12. Umamaheswari V, Palanichamy M, Murugesan V. Isopropylation of *m*-cresol over mesoporous Al-MCM-41 molecular sieves. *J Catal.* 2002;210:367–374.
13. Samolada MC, Grigoriadou E, Kiparissides Z, Vasalos IA. Selective o-alkylation of phenol with methanol over sulphates supported on γ-Al_2O_3. *J Catal.* 1995;152:52–62.
14. Sad ME, Padró CL, Apesteguía CR. Synthesis of cresols by alkylation of phenol with methanol on solid acids. *Catal Today.* 2008;133–135:720–728.
15. Karthik M, Tripathi AK, Gupta NM, Vinu A, Hartmann M, Palanichamy M, Murugesan V. Characterization of Co,Al-MCM-41 and its activity in the *t*-butylation of phenol using isobutanol. *Appl Catal A.* 2004;268:139–149.
16. Devassy BM, Shanbhag GV, Lefebvre F, Halligudi SB. Alkylation of *p*-cresol with *tert*-butanol catalyzed by heteropoly acid supported on zirconia catalyst. *J Mol Catal A.* 2004;210:125–130.
17. Sato S, Takahashi R, Sodesawa T, Matsumoto K, Kamimura Y. *Ortho*-selective alkylation of phenol with 1-propanol catalyzed by CeO_2-MgO. *J Catal.* 1999;184:180–188.
18. Velu S, Swamy CS. Selective C-alkylation of phenol with methanol over catalysts derived from copper-aluminum hydrotalcite-like compounds. *Appl Catal A.* 1996;145:141–153.
19. García L, Giannetto G, Goldwasser MR, Guisnet M, Magnoux P. Phenol alkylation with methanol: effect of sodium content and ammonia selective poisoning of an HY zeolite. *Catal Lett.* 1996;37: 121–123.
20. Yadav GD, Kumar P. Alkylation of phenol with cyclohexene over solid acids: insight in selectivity of O- versus C-alkylation. *Appl Catal A.* 2005;286:61–70.
21. Gagea BC, Parvulescu AN, Parvulescu VI, Auroux A, Grange P, Poncelet G. Alkylation of phenols and naphthols on silica-immobilized triflate derivate. *Catal Lett.* 2003;91:141–144.
22. Grabowska H, Mista W, Trawczynski J, Wrzyszcz J, Zawadzki M. A method for obtaining thymol by gas phase catalytic alkylation of *m*-cresol over zinc aluminate spinel. *Appl Catal A.* 2001;220:207–213.
23. Velu S, Sivasanker S. Alkylation of *m*-cresol with methanol and 2-propanol over calcined magnesium-aluminum hydrotalcites. *Res Chem Intermed.* 1998;24:657–666.
24. Bregolato M, Bolis V, Busco C, Ugliengo P, Bordiga S, Cavani F, Ballarini N, Maselli L, Passeri S, Rossetti I, Forni L. Methylation of phenol over high-silica beta zeolite: effect of zeolite acidity and crystal size on catalyst behavior. *J Catal.* 2007;245:285–300.
25. Ma Q, Chakraborty D, Faglioni F, Muller RP, Goddard WA, Harris T, Campbell C, Tang Y. Alkylation of phenol: a mechanistic view. *J Phys Chem A.* 2006;110:2246–2252.
26. Jansang B, Nanok T, Limtrakul J. Structure and reaction mechanism of alkylation of phenol with methanol over H-FAU zeolite: an ONIOM study. *J Phys Chem C.* 2008;112:540–547.
27. O'Connor CT, Moon G, Bohringer W, Fletcher JCQ. Alkylation of phenol and *m*-cresol over zeolites. *Collect Czech Chem Commun.* 2003;68:1949–1967.
28. Yadav GD, Thorat TS. Kinetics of alkylation of *p*-cresol with isobutylene catalyzed by sulfated zirconia. *Ind Eng Chem Res.* 1996;35: 721–731.
29. Santacesaria E, Grasso D, Gelosa D, Carra S. Catalytic alkylation of phenol with methanol: factors influencing activities and selectivities. I. Effect of different acid sites evaluated by studying the behavior of the catalysts: γ-alumina, nafion-H, silica-alumina and phosphoric acid. *Appl Catal.* 1990;64:83–99.
30. Madon RJ, Boudart M. Experimental criterion for the absence of artifacts in the measurement of rates of heterogeneous catalytic reactions. *Ind Eng Chem Fundam.* 1982;21:438–447.
31. Zhu XL, Lobban LL, Mallinson RG, Resasco DE. Tailoring the mesopore structure of HZSM-5 to control product distribution in the conversion of propanal. *J Catal.* 2010;271:88–98.
32. Fameth WE, Gorte RJ. Methods for characterizing zeolite acidity. *Chem Rev.* 1995;95:615–635.
33. Sad ME, Padró CL, Apesteguía CR. Study of the phenol methylation mechanism on zeolites HBEA, HZSM5 and HMCM22. *J Mol Catal A.* 2010;327:63–72.
34. Liu X, Liu M, Guo X, Zhou J. SO_3H-functionalized ionic liquids for selective alkylation of m-cresol with *tert*-butanol. *Catal Commun.* 2008;9:1–7.
35. Koros RM, Nowak EJ. A diagnostic test of the kinetic regime in a packed bed reactor. *Chem Eng Sci.* 1967;22:470.

36. Gunther WR, Duong Q, Roman-Leshkov Y. Catalytic consequences of borate complexation and pH on the epimerization of L-arabinose to L-ribose in water catalyzed by Sn-Beta zeolite with borate salts. *J Mol Catal A*. 2013;379:294–302.
37. Nie X, Liu X, Song C, Guo X. Bronsted acid-catalyzed tert-butylation of phenol, *o*-cresol and catechol: a comparative computational study. *J Mol Catal A*. 2010;332:145–151.
38. Yadav GD, Kamble SB. Synthesis of carvacrol by Friedel-Crafts alkylation of *o*-cresol with isopropanol using superacidic catalyst UDCaT-5. *J Chem Technol Biotechnol*. 2009;84:1499–1508.
39. Nie X, Liu X, Gao L, Liu M, Song C, Guo X. SO_3H-functionalized ionic liquid catalyzed alkylation of catechol with *tert*-butyl alcohol. *Ind Eng Chem Res*. 2010;49:8157–8163.
40. Ng S, Harris HG, Prausnitz JN. Henry's constants for methane, ethane, ethylene, propane, and propylene in octadecane, eicosane, and docosane. *J Chem Eng Data*. 1969;14:482–483.
41. Nitta M, Aomura K, Yamaguchi K. Alkylation of phenols. II. The selective formation of thymol from *m*-cresol and propylene with a γ-alumina catalyst. *Bull Chem Soc Jpn*. 1974;10:2360–2364.
42. Forissier M, Bernard JR. Deactivation of cracking catalysts with vacuum gas oils. In: Bartholomew CH, Butt JB, editors. *Catalyst Deactivation*. Amsterdam: Elsevier Science Publishers B.V.,1991: 359–366.
43. Nevicato D, Pitault I, Forissier M, Bernard JR. The activity decay of cracking catalysts: chemical and structural deactivation by coke. In: Delmon B, Froment GF, editors. *Catalyst Deactivation—Studies in Surface Science and Catalysis*, vol. 88. Elsevier Science B.V., 1994: 249–256.
44. Olson DH, Haag WO, Borghard WS. Use of water as a probe of zeolitic properties: interaction of water with HZSM-5. *Microporous Mesoporous Mater*. 2000;3536:435–446.
45. Malshe KM, Patil PT, Umbarkar SB, Dongare MK. Selective *C*-methylation of phenol with methanol over borate zirconia solid catalyst. *J Mol Catal A*. 2004;212:337–344.
46. Dixit L, Prasada TSR. Heats of adsorption of hydrocarbons on zeolite surfaces: a mathematical approach. *J Chem Inf Model*. 1999;39: 218–223.
47. Xu W, Miller SJ, Agrawal PK, Jones CW. Positive effect of water on zeolite BEA catalyzed alkylation of phenol with propylene. *Catal Lett*. 2013;144:434–438.

Manuscript received July 29, 2014, and revision received Sep. 28, 2014.